

Straight and kinked 90° partial dislocations in diamond and 3C-SiC

This article has been downloaded from IOPscience. Please scroll down to see the full text article.

2002 J. Phys.: Condens. Matter 14 12741

(<http://iopscience.iop.org/0953-8984/14/48/311>)

View [the table of contents for this issue](#), or go to the [journal homepage](#) for more

Download details:

IP Address: 171.66.16.97

The article was downloaded on 18/05/2010 at 19:12

Please note that [terms and conditions apply](#).

Straight and kinked 90° partial dislocations in diamond and 3C-SiC

A T Blumenau^{1,2,6}, C J Fall², R Jones², M I Heggie³, P R Briddon⁴,
T Frauenheim¹ and S Öberg⁵

¹ Theoretische Physik, Universität Paderborn, D-33098 Paderborn, Germany

² School of Physics, University of Exeter, Exeter EX4 4QL, UK

³ CPES, University of Sussex, Brighton BN1 9QJ, UK

⁴ Department of Physics, University of Newcastle, Newcastle upon Tyne NE1 7RU, UK

⁵ Department of Mathematics, University of Luleå, S90187, Luleå, Sweden

E-mail: blum@phys.upb.de

Received 27 September 2002

Published 22 November 2002

Online at stacks.iop.org/JPhysCM/14/12741

Abstract

Density-functional based calculations are used to investigate low energy core structures of 90° partial dislocations in diamond and 3C-SiC. In both materials dislocation glide is analysed in terms of kink formation and migration and the fundamental steps to kink migration are investigated. We find the C terminated core structure in SiC to be more mobile than the Si core. However, the Si partial is electrically active and this opens the possibility of recombination-enhanced glide under ionizing conditions or an enhanced mobility in doped material.

(Some figures in this article are in colour only in the electronic version)

1. Introduction

60° dislocations are common line defects in both diamond and SiC. They glide on {111} planes in diamond and 3C-SiC, and on the {0001} basal plane in the other SiC polytypes. In both materials they are known to dissociate into 90° and 30° Shockley partial dislocations separated by an intrinsic stacking fault [1, 2]. Further, the technologically relevant problem of *forward voltage degradation* in 4H-SiC PiN diodes is related to electrically active partial dislocations. Presumably in this process, extended stacking faults are developed by recombination-enhanced movement of the bordering partial dislocations [3].

This paper exclusively investigates the structure and motion of the 90° partial via a kink generation and diffusion mechanism. Kink formation and dislocation glide processes are by far the more complicated to model for 30° partials since they exist in double-period structures only.

⁶ Author to whom any correspondence should be addressed.

2. Theoretical methods

We use two computational methods with a different level of approximation to density functional theory (DFT): DFTB (density-functional based tight-binding method) and AIMPRO (*ab initio* modelling program). The DFTB method is a tight-binding method using a minimal basis of atomic orbitals (linear combination of atomic orbitals, LCAO). The two-centre Hamiltonian and overlap matrix elements are obtained from atom-centred valence electron orbitals and the atomic potentials from single-atom DFT calculations. Exchange and correlation contributions in the total energy as well as the core–core repulsion are taken into account by a repulsive pair potential. The latter is obtained by comparison with DFT calculations for selected reference systems [4]. The AIMPRO method uses the pseudopotentials of Bachelet *et al* [5] in combination with a Gaussian basis set and has been described in detail elsewhere [6]. This method requires greater computing resources and thus in this paper, geometrical optimization as well as the calculation of formation energies and barriers are carried out using DFTB with models containing at least 400 atoms. Comparison for smaller models gave good agreement between both methods.

3. Straight 90° partial dislocations

3.1. Core structures and energies

A unit cell is constructed by inserting a single dislocation into an infinite cylinder whose surface dangling bonds are hydrogenated. The dislocation is aligned with the axis of the cylinder and is periodic along the dislocation line. More than 100 Å of vacuum separates cylinders stacked on a square lattice. This supercell–cluster hybrid approach respects the periodicity of the dislocation along the line and avoids artificial dislocation–dislocation interactions which occur when a dipole is inserted into a supercell. The cylinders have a period twice that of the cubic lattice, $a_0[110]$, and have a radius $\sim 3.5a_0$. Thus the unit cell contains ~ 600 atoms. Structural relaxations are performed at the Γ point only and the surface was allowed to relax freely. In a recent paper we have shown, that—for the given size of our models—this approach is sufficient to give a good representation of the surrounding bulk crystal [7]. Figures 1 and 2 show the various relaxed core structures for the 90° glide partial in diamond and 3C-SiC, respectively. In each case we consider both the single-period (SP) and the double-period (DP) reconstruction. The latter was first proposed for silicon by Bennetto *et al* [8] and can be obtained from the SP structure by introducing alternating kinks. In SiC, one has to distinguish between those core structures which terminate with C atoms and those which terminate with Si atoms.

From linear elasticity theory it is known that the elastic energy contained in a cylinder of radius R around the dislocation depends logarithmically on the radius. The gradient of energy versus $\ln(R/\text{Å})$ can be obtained from the elastic constants, the line direction and the Burgers vector [9]. Figure 3 gives the corresponding plots of the atomistic formation energy for the two DP structures in SiC with respect to bulk SiC.

The dislocation energies for large R show the behaviour expected from using elasticity theory. These energies allow us to estimate the core energy. We find the energy of the carbon core to be about 0.6 eV Å^{-1} higher than the corresponding Si core. This is mainly due to the stretched C–C reconstruction bonds (15% compared to bulk diamond) whereas the Si–Si bonds assume an equilibrium length almost equal to that of bulk Si. For both diamond and SiC, the DP structures are lower in energy. However, the energy difference is rather small (diamond 170 meV Å^{-1} and SiC 90 meV Å^{-1}) and it is possible that both structures will co-exist.

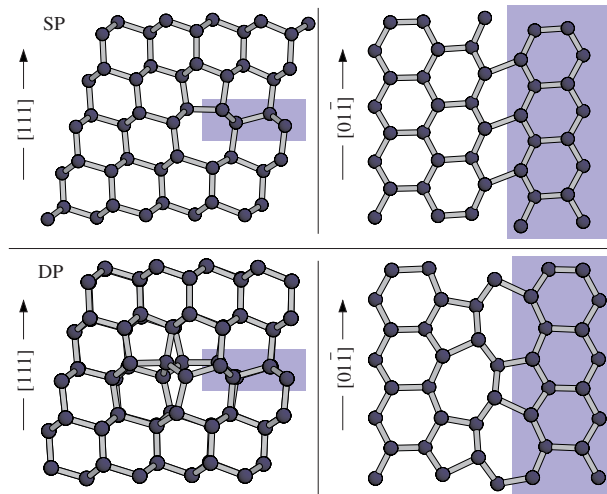


Figure 1. The relaxed core structures of the 90° partial in diamond. The intrinsic stacking fault area is shaded. The left and right panels show the view along the dislocation line and the projection into the glide plane, respectively. Upper panels: the SP core reconstruction. Lower panels: the DP core reconstruction.

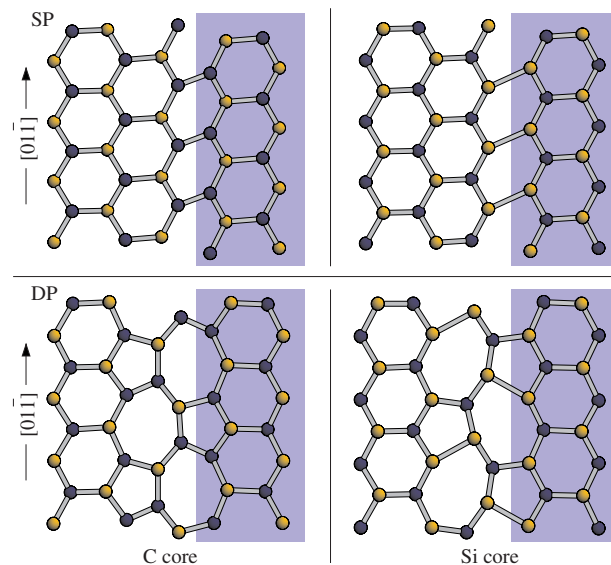


Figure 2. The relaxed core structures of the 90° partial in 3C-SiC. The intrinsic stacking fault area is shaded. All structures are projections into the glide plane. The left and right panels show the C-terminated core structure and the Si-terminated structure, respectively. Upper panels: the SP core reconstruction. Lower panels: the DP core reconstruction.

3.2. Electronic structure

The electronic structure of dislocations in diamond has been discussed in detail recently [10]. The 90° partial has been shown to induce only small changes in the electronic band structure and in particular no deep gap bands are formed. Here we focus on the electronic structure of

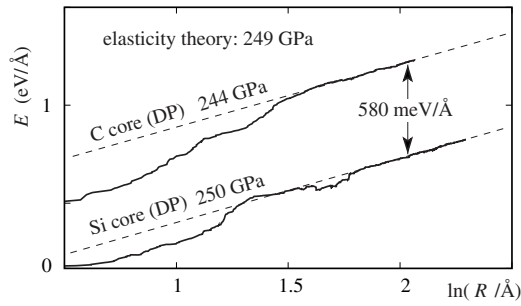


Figure 3. The formation energy of the DP 90° partials in 3C-SiC. The formation energy per unit length within a cylinder with radius R around the dislocation is plotted versus $\ln(R/\text{\AA})$. The broken lines are the linear fits in the limit $R \rightarrow \infty$ of elasticity theory. The energy integration within the respective cylinders around the dislocation was performed as the sum of atom-projected energies. The latter are easily obtained within the DFTB method. For details see [7].

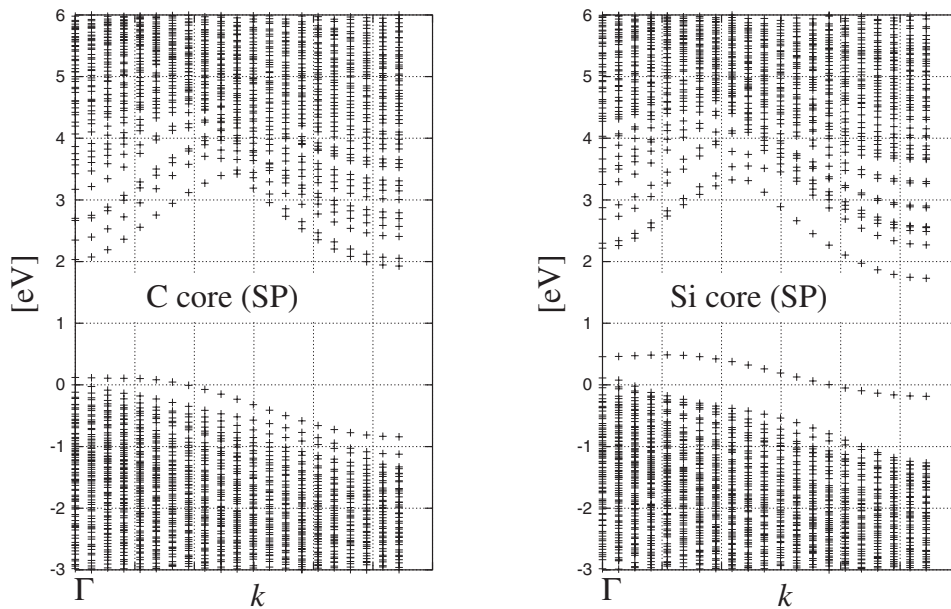


Figure 4. The electronic band structure of the SP 90° partials in 3C-SiC. The band structure is projected onto the direction in k space that corresponds to the dislocation periodicity along the line. Left: C-terminated core structure. Right: Si-terminated core structure.

dislocations in 3C-SiC. As can be seen in figure 4, only the Si core induces a deep band in the gap (AIMPRO). For a neutral dislocation the band is occupied and strongly localized at the very core region of the dislocation. This contrasts with the C core which exhibits little difference with bulk SiC.

4. Kinked dislocations and glide motion

Dislocation glide arises from an external stress acting on the dislocation, leading to the creation of kinks. When the stress is insufficient to overcome the Peierls barrier, kinks must be generated

by a thermal process and motion occurs by their migration along the dislocation line. In the case when obstacles (point defects and impurities) are not present, and for short dislocation segments, the velocity is controlled by the sum of the double kink formation energy $2E_f$ and the kink migration barrier W_m [9]:

$$v_{\text{disl}} \propto e^{-(Q-TS)/kT} \quad \text{with } Q = 2E_f + W_m. \quad (1)$$

For long segments, the activation energy is controlled by the sum of the single kink formation energy E_f and the kink migration barrier. In this paper we obtain the double kink formation energy by comparing the energies of a straight dislocation and one containing a double kink, in two hydrogen-terminated clusters (~ 400 atoms) with the same stoichiometry. Just as before the surface was allowed to relax freely. The double kink has a width of $a_0[110]$. To obtain E_k , the elastic interaction energy between the ends of the double kink has to be subtracted [9].

For SP structures in both C and Si partials in SiC, and the partial in diamond, we obtain $2E_f \approx 1$ eV. As shown in figure 5 for diamond (SP), the expansion of the double kink can be described as a succession of two-atom processes. To find the intermediate saddle point structure S, the elementary kink migration step was parametrized by the coordinates of each of two core (primary) atoms at the end of the kink projected onto the connecting line between their initial and final positions. Varying these two parameters independently yields a two-dimensional energy surface. The energy surface shown in figure 5 was obtained at 10×10 points in the two-dimensional parameter space by relaxing the whole structure subject to the constraint that the two primary atoms were constrained to lie in a plane perpendicular to the connecting line between the initial and final position. In the vicinity of S, the parameter mesh was refined by a factor of 10. In diamond we obtain a kink migration barrier of $W_m = 2.5$ eV. For SiC the migration barrier is 1.8 and 3.1 eV at the C and Si core, respectively (figure 6). Hence the C partial is more mobile than the Si one. The low value at the C core probably arises from the weak reconstruction of the partial which then allows kinks to form easily. Since similar processes are involved in the creation and movement of kinks in the DP structures, we expect qualitatively similar results.

In comparison with the earlier cluster AIMPRO results for SiC [11], we find a kink migration barrier about 0.4 eV higher. This might result from the use of a much larger cluster of atoms used here which models more accurately the stress response of the surrounding bulk material. In addition, in [11] the migration barrier was deduced from the barrier to double kink formation, rather than kink expansion as modelled here. The formation energy of the smallest double kink in the C partial is also 0.4 eV lower than that found in the present paper. A more striking difference is found for the Si partial. In this work we find the kink formation energy to be similar to that at the C core, whereas in [11] it is negligible. Nevertheless, both calculations conclude that the mobility of C partials should be higher than that of Si partials, and that the velocities of undecorated neutral partials is largely controlled by the kink migration energy.

5. Summary and conclusions

We have shown that the difference in energies between the single and DP reconstructions for 90° partials in diamond and SiC is almost negligible. This makes it likely that both structures will co-exist. Furthermore, in both materials, the glide of partials is dominated by the kink migration energy which is two to three times higher than the double kink formation energy. This assumes that the partials are neutral and are undecorated.

In SiC we find the glide activation energies Q for short dislocation segments to be 2.7 and 4.1 eV for C and Si partials, respectively. Thus the C core structure is thermally more mobile. Experimental results in 6H-SiC give $Q = 2.1\text{--}4.8$ eV [12, 13], very close to our results.

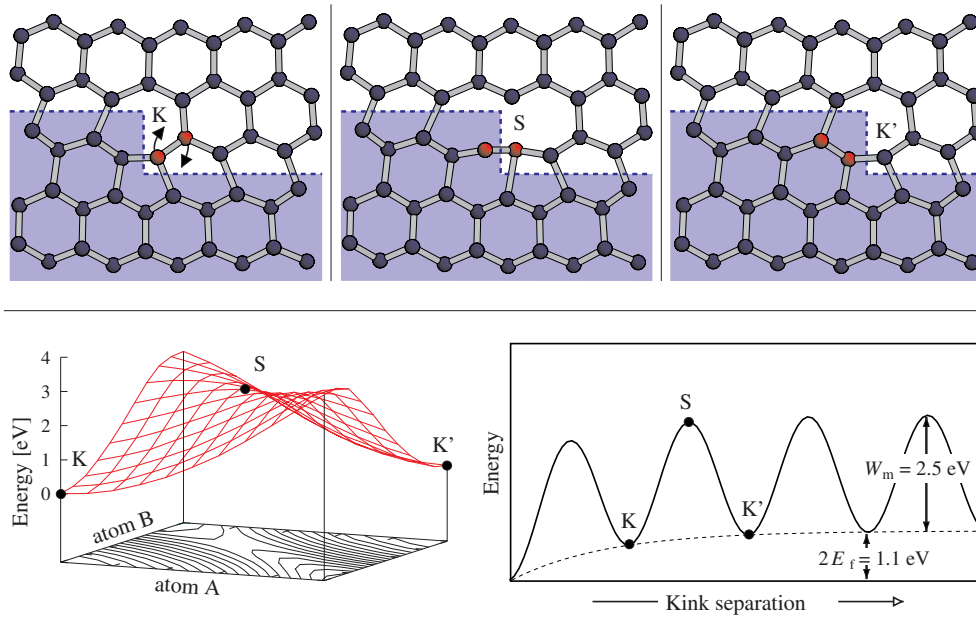


Figure 5. 90° dislocation glide in diamond. Top panels: the starting kink structure K, the saddle point structure S and the final kink structure K'. Bottom panels: formation energies and migration barriers of 90° dislocation glide in diamond. Left: Energy surface of a single migration step from K to K' via S. Right: energy versus kink separation in a double kink creation and subsequent migration process.

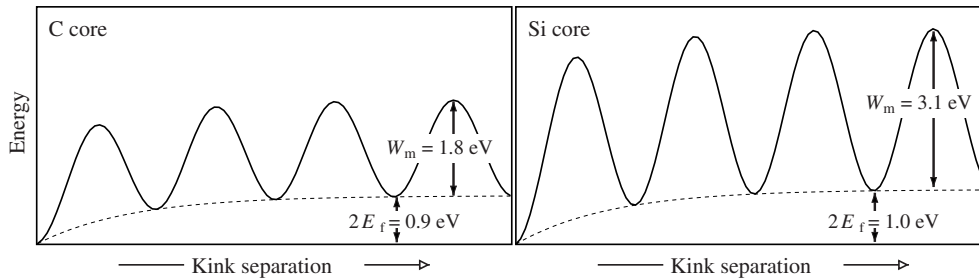


Figure 6. Formation energies and migration barriers of 90° dislocation glide in SiC. Left: C-terminated core structure. Right: Si-terminated core structure.

The carbon 90° partial in both diamond and SiC appears to be electrically inert. The Si partial in 3C-SiC appears, however, to be electrically active with a filled band low in the gap. This observation suggests that recombination enhanced glide of Si partials might occur under ionizing conditions and that the mobility of Si partials can be affected by doping. However, experimental observations [14] show that the Si partials in SiC are smooth whereas the C partials are zig-zagged, suggesting they are pinned by obstacles. In this case the glide process would not mainly be controlled by the formation and migration of kinks, but by the energy needed for the pinning and unpinning.

References

- [1] Pirouz P, Cockayne D J H, Sumida N, Hirsch Sir P and Lang A R 1983 *Proc. R. Soc. A* **386** 241
- [2] Samant A V, Zhou W L and Pirouz P 2000 *Phys. Status Solidi b* **222** 75
- [3] Lendenman H 2000 *UPD* (Japan: Nara)
- [4] Frauenheim T, Seifert G, Elstner M, Hajnal Z, Jungnickel G, Porezag D, Suhai S and Scholz R 2000 *Phys. Status Solidi b* **217** 41
- [5] Bachelet G B, Hamann D R and Schlüter M 1982 *Phys. Rev. B* **26** 4199
- [6] Briddon P and Jones R 2000 *Phys. Status Solidi b* **217** 131
- [7] Blumenau A T, Heggie M I, Fall C J, Jones R and Frauenheim T 2002 *Phys. Rev. B* **65** 205205
- [8] Bennetto J, Nunes R W and Vanderbilt D 1997 *Phys. Rev. Lett.* **79** 245
- [9] Hirth J P and Lothe J 1982 *Theory of Dislocations* 2nd edn (New York: Wiley)
- [10] Fall C J, Blumenau A T, Jones R, Briddon P R, Gutiérrez-Sosa A, Bangert U, Mora A E, Frauenheim T, Steeds J W and Butler J E 2002 *Phys. Rev. B* **65** 205206
- [11] Sitch P K, Jones R, Öberg S and Heggie M I 1995 *Phys. Rev. B* **52** 4951
- [12] Fujita S, Maeda K and Hoyodo S 1987 *Phil. Mag.* **A 55** 203
- [13] Samant A V, Zhou W L and Pirouz P 1998 *Phys. Status Solidi a* **166** 155
- [14] Ning X J and Pirouz P 1996 *Inst. Phys. Conf. Ser.* **142** p 449